

TEAM - Transmission of Epidemic Among Membranes

Sandro Erba^a,^{*}, Giuditta Franco^b, Francesco Reiff^b, José M. Sempere^c, Claudio Zandron^a

^a Department of Computer Systems and Communication, University of Milano-Bicocca, Milan, Italy

^b Department of Computer Science, University of Verona, Verona, Italy

^c VRAIN, Universitat Politècnica de València and VALGRAI, Valencia, Spain

ARTICLE INFO

Dataset link: <https://github.com/francireiff/TEAM>, Italian Civil Protection Department repository

Keywords:

Behavioral epidemiology
Distributed computing
Infection diffusion
Massive parallelism
Population dynamics

ABSTRACT

The COVID-19 pandemic has underscored the crucial role of computational simulation in understanding, predicting, and controlling infectious disease dynamics, as well as supporting data-driven decision-making in public health. Within this context, the biologically inspired membrane computing has been shown to be promising for modeling complex epidemiological systems, due to its population-based inherent parallelism and compartmental structure.

Two models stand out for their complementary strengths among the existing works that adopt this paradigm. One, known as LOIMOS, focuses on detailed representations of infection and symptom progression, offering a biologically rich modeling of disease stages. The other, referred to as MVT, introduces behavioral dynamics, allowing individuals to adapt their actions based on perceived risk, personal willingness to vaccinate, and inter-provincial mobility preferences.

This work combines the core ideas of LOIMOS and MVT into a unified simulation framework, referred to as TEAM (Transmission of Epidemic Among Membranes), which integrates biological accuracy with behavioral flexibility. The goal is to create a general-purpose model adaptable to various infectious diseases beyond COVID-19, usable as a decision support system. Central challenges included resolving formal and structural differences between the two source models and harmonizing their rule-based dynamics.

1. Introduction

Membrane computing is a branch of natural computing inspired by the structure and function of biological cells [1–3], through the metaphor of nested membranes and chemical reactions occurring within compartments [4].

P systems (introduced by Gheorghe Păun [5]) offer an inherently parallel and non-deterministic framework [6] that has attracted interest from both fields of theoretical computer science and systems biology [7]. Each membrane defines a region containing multisets of objects (representing chemical substances) and is subject to evolution rules that govern transformations, communications, and structural operations.

Various classes of P systems have been advanced in the literature, while P systems with active membranes are particularly expressive [8,9]. They extend the basic framework by introducing additional features such as membrane polarization, membrane division, and dissolution, enabling dynamic structural changes and enhanced computational power [10]. Division rules are particularly powerful, by allowing membranes to duplicate together with their contents. This feature enables exponential workspace growth, a critical asset in solving computationally hard problems such as the HPP and SAT [11–13].

Recent advancements in membrane computing have introduced significant refinements to the semantics of evolution rules, enabling more expressive and biologically realistic models. To provide finer control over the application of rules, three key mechanisms have been proposed:

- Input Population Percentage, which specifies the proportion of objects or membranes to which a rule is applied, enabling partial or population-level interactions;
- Rule Priority Index, which resolves conflicts between applicable rules based on their relative precedence, allowing deterministic selection;
- Rule Probability, which assigns a likelihood to rule execution when given conditions are met, by introducing controlled non-determinism and reflecting the probabilistic nature of many biological processes.

While expanding the model expressive power, these mechanisms remain consistent with the foundational principles of membrane computing, namely local interactions and rule-based rewriting.

* Corresponding author.

E-mail address: s.erba9@campus.unimib.it (S. Erba).

Some works have employed P systems to simulate epidemiological phenomena and the spread of infectious diseases under various conditions [14–18]. Building upon these foundations, we here introduce the TEAM epidemiological model, which extensively incorporates the three features above. We propose this model with the main aim to integrate the strengths and to tune or eliminate the limits of two prior recent models of the literature, LOIMOS [14] and MVT [15], into a unified framework, that enhances flexibility and expressiveness in simulating infection diffusion processes through membrane computing.

LOIMOS is a Greek word meaning pestilence, which more figuratively recalls pestilent fellows. It is the name for the epidemiological model developed at the Universitat Politècnica de València, which introduces a rich biological layer and a predictive statistical structure. In this context, the LOIMOS simulator should not be confused with another agent based tool from the literature sharing the same name.¹ It models epidemiological states in detail, assigning individuals to a broader set of location types while tracking a finer granularity of attributes, such as age group, viral load, symptom severity, and immune status. Infection in LOIMOS involves thousands of rules and complex object dynamics, where individuals generate and interact with virus, antiviral, specialized immune elements, and further components. In TEAM, these mechanisms are partially simplified in order to retain the main epidemiological dynamics while reducing the number of rules and improving the manageability of the simulation model. In LOIMOS, disease progression is influenced by both viral load and immune efficiency, producing various symptomatic trajectories, ranging from home isolation to hospitalization or ICU admission, each with associated recovery or mortality probabilities. LOIMOS also models four distinct infection types based on combinations of innate or acquired immunity and symptom intensity, reflecting more nuanced biological variability. LOIMOS enjoys realistic features and nice system properties, and achieves notable simulation results reported in [16,19]. In TEAM, some of these distinctions are abstracted into a smaller set of epidemiological states to obtain a more compact rule system while preserving the main behavioral patterns of the disease progression.

MVT is a rule-based simulator of disease spread across provinces implemented in Python. The name MVT reflects the collaborative work among the universities of Milano-Bicocca, Verona, and Trieste. In MVT, the population is distributed across multiple provinces among a limited set of location types: schools, workplaces, hospitals, and common areas. Each individual carries structured attributes including age, mobility data, and epidemiological status, while infection evolves according to simplified disease phases: latent period, active infection, and immunity. Behavioral adaptation [20] is a main feature of this approach, indeed it plays a central role, with individuals responding to local infection prevalence by altering movement patterns and risk behaviors, a mechanism captured by newly introduced Caution Parameter. This model basically integrates disease dynamics with geographic mobility, enabling exploration of how different vaccination strategies, different social restriction rules, and different behavioral responses, affect outcomes in the population. Successful simulations of this model among provinces of the Lombardy region in Italy are presented in [21].

MVT and LOIMOS provide complementary insights: the former focuses on adaptive behavior and geographic mobility, while the latter models immune response and symptomatology in greater biological detail. These models serve as a conceptual and technical foundation for TEAM, the unified framework presented in this paper. The name is inspired by the active collaboration between University of Milano Bicocca, Verona, and Universitat de València.

Membrane computing applied to epidemiology, as described above, produces what we can consider agent-based models (ABMs) [22,23]. These models have gained greater prominence in recent years, given

that they capture aspects such as dynamic interaction that other more classic models, such as temporal and compartmental models like SEIR (Susceptible–Exposed–Infectious–Recovered) cannot reflect. Furthermore, other approaches like network-based models are highly dependent on the network topology initially imposed, although in some studies this effect has been mitigated by using dynamically evolving networks [24]. Agent-based models emphasize individual-level heterogeneity, localized interaction, and adaptive behavior [22]. In recent years, ABMs have gained greater prominence, especially in the wake of the global crisis caused by COVID-19 [25]. These models have been shown to be ideal for the design of computational simulators that provide explainability, scalability, and flexibility.

Membrane computing, through P systems, provides virtual agents like objects with mobility. The regions defined by a P system have their particular rules of behavior. So, the compartmentalized structure of regions in a P system is capable of establishing different levels of infection that affect the global behavior of the model. The dynamics of these regions can be established by active rules of modifying the regions by fusion, deletion and duplication of membranes. For all these reasons, our proposal can be considered an agent-based with a dynamic network model.

From an even broader perspective, our work is part of the extensive literature focused on coupled infection-behavior dynamics, where the interplay between epidemic spreading and adaptive human behavior has been investigated [26], namely through evolutionary game-theoretic formulations of behavior-driven epidemic models [27]. Although this is a basin of inspirations for possible extensions of our current work, one main characterization and difference of our approach in the context of evolutionary vaccination game theory is that we adopt an implicit (vs explicit) behavior class of modeling, by integrating the dynamical concept of human behavior within the framework of Membrane Systems, where a rule-based mechanism is designed to qualitatively reproduce observed dynamics and predict new ones.

In the next sections, we present the source model and its simulator. Section 2 namely introduces the proposed model, detailing its rules for infection, contagion, symptoms, movement, recovery, and behavior. Section 3 describes the simulation scenario and implementation, including scalability analysis, infection generalization, and the database integration. Section 4 presents the validation of the model, reporting and discussing the results through graphical analyses and the impact of key variables. Section 5 concludes the paper and outlines potential future developments.

2. Model definition

TEAM model is defined as a cell-like P system with active membranes without polarization, formally described by the tuple:

$$\Pi = (V, H, \mu, w_1, w_2, \dots, w_m, R) \quad (1)$$

where:

1. V is the alphabet of objects. Each membrane contains objects, represented with multisets to map strings of symbols onto an alphabet. For a list of the main objects contained in V , please refer to Table 1;
2. H is the alphabet of labels for membranes. They have a type and a label to distinguish them from different membranes of the same type. More info can be found in Table 2;
3. μ is the initial membrane structure, of degree m , with all membranes labeled with elements of H . A membrane with label h is represented as $[\]_h$;
4. w_i are strings over V specifying the multiset of objects initially in the i th regions defined by μ .
5. R is a finite set of evolution rules.

¹ *Loimos: epidemic diffusion simulation code*, GitHub repository, Available at: <https://github.com/loimos/loimos>.

The membrane structure is tree-like: at the top is the skin membrane, which contains all provinces. Each province includes a variety of places such as houses, hospitals, schools, and more, each with a limited capacity. Individuals, modeled as membranes themselves, move between these places according to rules that reflect behavior and epidemiological state.

Each place serves a specific function: houses host families; hospitals and ICUs treat severe infections; schools, workplaces, and leisure centers capture daily routines; common areas model transit and crowded indoor environments. The leisure center represents both open and closed public spaces, varying in infection risk depending on time and use.

Embedded within places, individuals never leave the system but move through its membrane structure via movement rules that simulate interactions in a population. Every membrane carries objects that define its characteristics. Each place tracks local infection levels via an object ϕ indicating the number of infected individuals present, which directly determines the probability of contagion.

Objects within membranes represent information, control behavior, and enable evolution through rewriting rules.

Rules are described in the following, according to the process they control in the whole epidemiological dynamics. Each evolution rule $\alpha \xrightarrow{p,q} \beta$ has a precondition α , a postcondition β , where $\alpha, \beta \in V$, and a parametrized application guided by a couple of parameters p and q . The first parameter $p \in [0, 1]$ is a probability value that models the stochastic simulation of the systems, while the second parameter $q \in \mathbb{N}$ represents the value of a priority relation defined over the rules for the application order. This allows P systems to be effectively used in probabilistic modeling of biological networks, as shown in [28]. Therefore, it is a (parametrized, by the probability and the priority relation values) Markov model, since the next state depends deterministically on the current one, by the corresponding probabilistic rules application.

Table 1 reports the set of objects contained within an individual, together with their corresponding domains. Each of these objects belongs to the alphabet V . The multiplicity of each object within an individual encodes the quantity or the intensity of the corresponding attribute. For quantitative entities, such as the viral load v_1 or the time variable *hour*, multiple copies of the same object represent higher values (e.g., increased viral load or a later time of the day). This representation follows the standard formalism of membrane computing, where multiplicity is naturally handled through multiset rewriting and parallel rule application.

For variables defined over enumerated domains, such as *age* and *st*, the multiplicity of the corresponding objects determines the class membership of the individual. In particular, the multiplicity of *st* encodes the epidemiological state, with values 1, 2, 3, and 4 corresponding to S, E, I, and R, respectively. Furthermore, J_1 and J_2 denote subcategories of infected individuals (state I) characterized by severe and critical symptom level. For instance, an individual containing one occurrence of *age* and four occurrences of *st* represents a young recovered individual.

Table 2 summarizes the membranes defined in the model, specifying for each of them the corresponding label, capacity (computed for a reference scenario with 25,000 individuals and 12 provinces), cardinality, and semantic interpretation.

The object ϕ^x , with $x \in \{0, \dots, n\}$, where n denotes the population size, is associated with each place membrane and represents the number of infected individuals currently present within that membrane. This quantity is used to regulate and model the infection rates within each place membrane.

SEJIRS epidemiological model

Before describing TEAM in detail, we first outline how the progression of infections is represented in the simulator. Several levels of abstraction exist for modeling the lifecycle of a disease. Among the

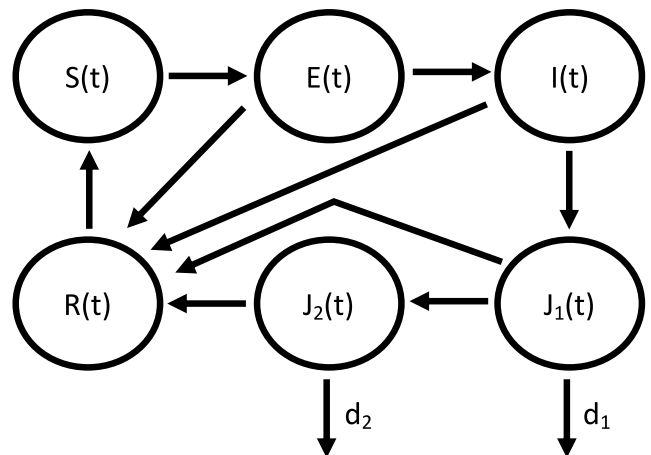


Fig. 1. SEJIRS model. Flow of individuals across classes of the SEJIRS model.

simplest and most widely used are the SIR model [29] and the SEIR model, described in [30] together with other similar approaches.

In this type of epidemiological formulation, each letter represents a possible compartment of the model. In the SIR model, individuals transition from Susceptible to Infected and finally to Recovered. The SEIR model extends this structure by introducing the Exposed class, which represents the latent period during which an individual is infected but not yet infectious.

More recently, more detailed epidemiological models have been proposed, such as SEIRQJ and SIDARTHE, originally developed to study SARS dynamics. These models introduce additional compartments to capture more refined aspects of disease progression. We do not discuss these models in detail here and refer the reader to Table 3 for a brief summary of their main characteristics.

Building on the ideas proposed in these works, the progression of the disease in TEAM follows an epidemiological model called SEJIRS, illustrated in the state diagram in Fig. 1.

Individuals start in the susceptible state S and, after exposure, enter the latent period state E , where they carry the infection but are not yet infectious. They may then progress to the infectious state I , where transmission to other individuals becomes possible and symptoms may appear. If symptoms worsen, individuals move to states with increasing severity: J_1 (moderate symptoms, typically isolated or hospitalized) and J_2 (severe symptoms requiring intensive care). Individuals in J_1 and J_2 have probabilities of death d_1 and d_2 , respectively, with $d_2 > d_1$. Individuals can recover and enter the R state, where they experience temporary immunity before eventually returning to the susceptible state S . Deaths are recorded as an output of the model rather than represented as an explicit compartment.

Infection rules

Infection depends on the location, the number of infected individuals, individual status, and contextual factors. The general form is:

$$[st^1]_{ind_j}, [st^3]_{ind_i}, \phi \longrightarrow [st^2, v_1^5]_{ind_j}, [st^3]_{ind_i}, \phi \quad (2)$$

In the precondition, individual j is in a healthy state while individual i is infected; in the postcondition, individual j transitions to the exposed state and receives an initial viral load represented by five v_1 objects. The rule is applied with probability

$$p = \beta \cdot \frac{\phi}{N} \cdot \psi(M),$$

where β is the base infection rate that depends on the membrane type, ϕ is the number of infected individuals in the location, N is the total number of individuals in the location, and $\psi(M)$ is a decreasing function modeling awareness of contagiousness [15].

Table 1
Main objects, the domain of their multiplicity, and the attributes associated with individuals in the TEAM model. Each of those objects are elements of V .

Object	Domain	Meaning
hm^x	$x \in H$	Identifier of the home membrane of the individual
hp^x	$x \in \{0, \dots, n\}$	Home province of the individual, where n is the number of simulated provinces
dp^x	$x \in \{0, \dots, n\}$	Destination province of the individual, where n is the number of simulated provinces, denotes the region in which the subject will move during their routine
$hour^x$	$x \in \{0, \dots, 23\}$	Current hour of the day
day^x	$x \in \{0, \dots, d\}$	Current simulation day, where d is the total number of simulated days
v_1^x	$x \in \{0, \dots, 1000\}$	Units of viral load, the multiplicity models the intensity level
$antiv^x$	$x \in \{0, \dots, 1000\}$	Units of non-specialized antivirus, the multiplicity models the intensity level
$antivesp^x$	$x \in \{0, \dots, 1000\}$	Units of specialized antivirus, the multiplicity models the intensity level
hdl^x	$x \in \{0, \dots, 7\}$	Number of hospitalization days left before the end of the health care period
vcc^x	$x \in \{0, 1\}$	Vaccination status indicating whether the individual is vaccinated
sym^x	$x \in \{1, 2, 3, 4\}$	Symptom severity level, larger values correspond to more severe symptoms
age^x	$x \in \{1, 2, 3\}$	Age group associated with an individual, where 1 \rightarrow <i>young</i> , 2 \rightarrow <i>adult</i> , 3 \rightarrow <i>elderly</i>
st^x	$x \in \{1, 2, 3, 4\}$	Epidemiological status of the individual, where 1 \rightarrow S , 2 \rightarrow E , 3 \rightarrow I , 4 \rightarrow R . Additional states J_1 and J_2 depend on symptoms.

Table 2
Membranes of the TEAM model. The domains are related to a simulation with a population of 25000 and 12 provinces. The capacities marked with an asterisk (*) are fixed for all runs.

Membrane	Label	Capacity	Domain	Meaning
Skin	$[\]_{SKIN_i}$	12	$i = 1$	The unique top-level membrane containing all and only the provinces of the model
Province	$[\]_{PR_i}$	780	$i \in \{1, \dots, 12\}$	Membranes representing the provinces; each contains all place membranes defined below
Common Area	$[\]_{CA_i}$	1041	$i \in \{1, \dots, 12\}$	One per province; gathers individuals in crowded environments. Movements across provinces lead to the corresponding Common Area
School	$[\]_{S_i}$	300*	$i \in \{1, \dots, 12\}$	Membranes hosting young individuals during daily school activities
Hospital	$[\]_{H_i}$	150*	$i \in \{1, \dots, 12\}$	Membranes hosting individuals with severe symptoms requiring medical care
ICU	$[\]_{ICU_i}$	1*	$i \in \{1, \dots, 48\}$	Isolated membranes hosting individuals with critical symptoms requiring intensive care
Workplace	$[\]_{W_i}$	200*	$i \in \{1, \dots, 96\}$	Membranes representing workplaces, hosting adult individuals during daily working hours
Leisure Center	$[\]_{LC_i}$	200*	$i \in \{1, \dots, 192\}$	Membranes representing leisure locations visited in the evening and during weekends
Home	$[\]_{HM_i}$	$\{1, \dots, 6\}$ *	$i \in \{1, \dots, 9000\}$	Membranes representing households with variable capacity, associated with individuals
Individual	$[\]_{ind_i}$	3000	$i \in \{1, \dots, 25000\}$	Membranes representing individuals, which move across place membranes and contain the objects defined in Table 1

Table 3
Comparison of epidemiological models.

Model	Key feature	Examples of diseases
SIR [29]	Permanent immunity	Measles, chickenpox
SEIR [30]	Permanent immunity, latent period	COVID-19, Ebola
SIS [31]	No immunity	Common cold
SIRS [31]	Temporary immunity	Influenza, COVID-19
SEIS [32,33]	No immunity, latent period	Tuberculosis
SEIRS [34]	Temporary immunity, latent period	Dengue fever
SEIRQJ [35]	Asymptomatic, quarantined, isolated individuals	2003 SARS
SIDARTHE [36–39]	Undiagnosed cases, varying symptom severity	COVID-19

Table 4
Rules governing immune response and viral load dynamics, ordered by decreasing priority.

Precondition	Probability	Postcondition	Description
$antiv^{200}, v_1^{200}$	0.012	$antivesp,$ $v_1_{ino},$ $antiv^{199},$ $v_1^{199},$ $sint^{200}$	The individual's antibodies fight the disease, and a new specialized antibody is created. The probabilities for applying this rule depend on the individual's state of health
$antivesp, v_1$	1	$antivesp,$ $v_1_{ino},$ $sint$	Each specialized antibody fights the infection, generating harmless viruses
$antiv, v_1$	0.001	$antiv,$ $v_1_{ino},$ $sint$	Each non-specialized antibody fights against the infection with a lower probability
v_1	0.035	$v_1^2, sint$	Viruses not occupied by the other rules are free to grow
v_1	1	$v_1, sint$	Symptoms increase according to the viral load present, even if the v_1 elements follow no specific rule

Viral load rules

The rules in Table 4 are some of the many defined in TEAM, selected for their explanatory value in illustrating the management of viral load within an individual. They are listed in order of decreasing priority. For a definition of the objects listed in the following tables and their domains, please refer to Table 1. Note that each of those evolution rules generates a certain number of symptom objects, useful for the next block of rules, depending on how many virus objects are involved in the preconditions of the rule.

Symptoms rules

Each individual has a symptom status object sym^x , with $x \in \{1, 2, 3, 4\}$:

- sym^1 : the host has no symptoms, and may be or may not be infected
- sym^2 : the host has mild symptoms, may be or may not realize he is infected
- sym^3 : the host has severe symptoms and needs hospitalization
- sym^4 : the host has critical symptoms and needs ICU

The rules in Table 5 manage system variables related to symptoms, where the probability of symptom growth is derived from the LOIMOS model and later balanced after integration with MVT.

In particular, the fourth rule introduces a threshold-based mechanism: when the number of *sint* objects reaches a fixed value of 700, the system transitions to a high viral load state, represented by *cont*. This mechanism is inherited from the LOIMOS model and should be regarded as a simplification, rather than a clinically accurate representation. It does not imply a direct or clinically validated correlation between viral load and symptom severity, but rather provides a practical abstraction to trigger state transitions.

Movement rules

Movements simulate daily routines or inter-provincial transfers. All movements are handled by membrane mobility rules.

$$[[[hp^k, dp^l]_{ind}]_{HM}]_{PR_k} \longrightarrow [[[hp^k, dp^l]_{ind}]_{CA}]_{PR_l} \quad (3)$$

where *ind* represents an individual who wants to move from province *k* to province *l*, and *HM* and *CA* denote, respectively, the home membrane of the starting province and the common area of the destination province. The probability of applying this rule depends on the epidemiological situation of the destination province, but it will be 0 if the movement from *k* to *l* is not scheduled in the routine of *ind* for the given hour and day. Other movement rules handle transitions within the same province, such as commuting between places (e.g., home

and workplace), but follow the same idea as the one shown. These movement rules bring the model to life, allowing individuals to follow their own routines.

Recovering rules

Having described how an individual becomes infected, how the disease evolves, and how symptoms develop, we now present how recovery occurs. In all cases, a recovered individual gains immunity for 180 days. There are three ways to recover:

- Recovery through hospitalization: infected individuals with severe or critical symptoms (sym^3 or sym^4) have a probability of 0.03 (for hospital) or 0.05 (for ICU) per hour of being admitted to a suitable facility, if available in the region. If already hospitalized and symptoms worsen to critical (sym^4), the individual is moved directly to ICU. ICU availability is limited, so simulations must be correctly parametrized. Once admitted, a 7-day recovery cycle begins. The same cycle applies to ICU transfers, as hospitalization days are shared across facilities.
- Recovery through specialized antivirus: if the individual accumulates enough specialized antivirus objects, they are considered cured. The production rate and healing threshold of specialized antivirus are critical parameters that have undergone a tuning phase.
- Recovery by zeroing the viral load: even without hospitalization or a full antibody response, if specialized and non-specialized antivirus reduce the viral load to zero, the individual recovers.

Behavior

To enhance realism, TEAM includes individual behaviors that influence epidemic dynamics, inspired by MVT. These behaviors add heterogeneity and decision-making capacity to individuals, preventing uniform reactions across the population and improving the realism of the simulation [20]. Four main behavioral features are implemented:

- Prudence Parameter: models the tendency of individuals to modify their behavior when experiencing symptoms. In particular, mildly symptomatic individuals (sym^2) may choose to stay home depending on their prudence level, so a higher *PP* reduces the probability of going out while infected. While this parameter captures individual decision-making, it represents an aggregate effect that also reflects external influences such as public awareness and information availability. For instance, in the early stages of a novel disease, lower values of *PP* may reflect limited knowledge and risk perception, whereas higher values may emerge in contexts with widespread awareness or strong public health messaging.

Table 5
Rules governing symptom progression and viral load effects, ordered by decreasing priority.

Precondition	Probability	Postcondition	Description
$sym^1, cont$	1	sym^2	Transition from no symptoms to mild symptoms due to sustained high viral load
$sym^2, cont$	$1.5 \cdot 10^{-3}$	sym^3	Transition from mild symptoms to severe symptoms due to sustained high viral load
$sym^3, cont$	10^{-3}	sym^4	Transition from severe symptoms to critical symptoms due to sustained high viral load
$sint^{700}, flag$	1	$cont, flag$	When there are 700 <i>sint</i> objects, this rule consumes the <i>flag</i> object and generates the <i>cont</i> object, which represents a high viral load state
$sym^x, cont$	1	$sym^x, cont$	If the <i>cont</i> object is present and the host does not worsen, the current state is maintained
sym^x	1	sym^1	If there is no <i>cont</i> object, the viral load is not dangerous, so the host is cured and the symptoms disappear
<i>sint</i>	1	λ	The object <i>sint</i> is used to know how many objects v_1 there were in a previous step. If they are not used, this rule deleted them
$[sym^3]_{ind}$	$1.6 \cdot 10^{-5}$	λ	An individual with severe symptoms can trigger a dissolving rule, resulting in death
$[[sym^4]_{ind}]_{ICU}$	10^{-4}	$[\lambda]_{ICU}$	An individual with critical symptoms who is admitted to the ICU may trigger a dissolving rule, resulting in death
$[[sym^4]_{ind}]_{HM}$	$2 \cdot 10^{-4}$	$[\lambda]_{HM}$	An individual with critical symptoms who stays at home may trigger a dissolving rule, resulting in death

Table 6
Movement probabilities for each routine rule in the algorithm. ϕ_d and N_d are the number of infected individuals and total population at the destination membrane. *PP* is the Prudence Parameter.

Code line	Pseudocode rule	Age group	Symptom	Probability
Line 16	Move between provinces	Young, Adult	sym^1	$1 - \frac{\phi_d}{N_d}$
			sym^2	$\left(1 - \frac{\phi_d}{N_d}\right) (1 - PP)^2$
Line 16	Move between provinces	Elderly	sym^1	$0.17 \cdot \left(1 - \frac{\phi_d}{N_d}\right)$
			sym^2	$0.17 \cdot \left(1 - \frac{\phi_d}{N_d}\right) (1 - PP)^2$
Line 17	Move to workplaces	Adult	sym^1	1
			sym^2	$(1 - PP)^2$
Line 18	Move to schools	Young	sym^1	1
			sym^2	$(1 - PP)^2$
Line 19	Move to leisure centers	Elderly	sym^1	0.04
			sym^2	$0.04 \cdot (1 - PP)^2$
Line 21	Move back home	All	sym^1, sym^2	1

- Likelihood to Change Province: individuals avoid traveling to provinces with high infection rates. The probability of inter-provincial movement decreases with the proportion of infected people in the destination area, discouraging mobility toward high-risk zones. The number of individuals not predisposed to change provinces in their routine is a fixed parameter called Same Province Percentage, which can be set during simulation creation.
- Caution Factor: as infections rise, people become more cautious. This is modeled through a decreasing function that reduces contagion probability as the infection rate increases.
- Vaccination Will: the willingness to get vaccinated increases with perceived risk, based on infection prevalence. Individuals are vaccinated based on a probability modulated by a behavioral function. Each vaccinated person receives a randomly assigned vaccine efficacy and a corresponding protection duration.

3. Scenario and simulations

TEAM was developed using an Object-Oriented Programming (OOP) approach, enabling a clear and efficient translation of the membrane computing paradigm into code. This design choice proved particularly suitable for preserving the hierarchical organization of the starting

MVT model, while ensuring a high degree of flexibility, compared to existing frameworks tailored to membrane computing such as LOIMOS and P-Lingua [40].

In the TEAM simulator, individuals are modeled as objects with attributes representing their health status. The multiplicity of objects in membrane computing is conceptually used to encode quantitative properties, such as viral load or time progression. In the implementation, however, this is not realized through explicit object duplication; instead, it is efficiently handled via attributes within the object-oriented structure, avoiding unnecessary memory overhead while preserving the formal semantics at an abstract level.

The rewriting rules of membrane computing are implemented as methods, and a strict constraint is applied: no attribute can change more than once per simulation step, in accordance with membrane computing semantics. Rule application respects both priority and probability, and membrane hierarchy ensures organizational consistency (e.g., provinces contain places, which contain individuals).

Python was used as the programming language due to its simplicity, data handling capabilities, and support for OOP. The simulation progresses in discrete time steps, each representing one hour. At each step, every object can apply one rule, and a new configuration is generated.

The system halts when a predefined number of steps (entered as input, in days) is reached.

To broaden the simulator usability, a key development was the creation of a Graphical User Interface (GUI) using Python Tkinter library. The primary goal of the GUI is to make the sophisticated model accessible to researchers and officials who are not programming experts, such as those in epidemiology or public health. The interface organizes the numerous simulation parameters—from population and behavioral factors to lockdown rules—into a clear, tabbed layout. To further aid usability, it incorporates informative tooltips that explain the function of each parameter. Upon completing a run, the GUI presents the results, including key data and plots, directly within an integrated output panel, facilitating immediate analysis. This feature removes the barrier of direct code manipulation and establishes the simulator as a practical tool for flexible scenario testing. The complete source code for the TEAM simulator is publicly available.²

Scalability of the scenario

A fundamental aspect of this work is the generalization of the model in terms of both structure and application. The initial simulators were tailored specifically to COVID-19 and did not have an easily editable scenario. For example, LOIMOS required pre-defined input files for membranes, making structural changes cumbersome, while MVT used a fixed number of regions, limiting flexibility.

TEAM introduces a dynamic system that allocates place membranes based on realistic capacity assumptions. These capacities are now decoupled from hardcoded values and instead reflect typical structural limits observed in real-world contexts. This change ensures a more coherent relationship between population size and the number of available facilities.

Particular attention was given to the modeling of healthcare structures, where capacity constraints are critical for simulating scenarios such as hospital saturation.

The new approach enables the simulator to recreate more realistic and flexible settings, allowing the exploration of scenarios in which healthcare resources become limited. In particular, the model includes a mechanism to detect when hospital or ICU capacity approaches saturation (i.e., above 90%) and explicitly flags this condition during the simulation.

The model does not implement any triage or admission policy, nor does it make decisions regarding patient prioritization. Instead, it only signals the occurrence of critical situations in which healthcare capacity is reached or nearly reached. Once such a condition is detected, the simulation output should be interpreted with caution, and any decision-making should be carried out in consultation with domain experts.

If the simulation is allowed to continue beyond this point, it represents a hypothetical uncontrolled scenario in which resource allocation is not actively managed, for example, following a simple first-come, first-served logic. As such, the resulting outcomes, including increased mortality, should be understood as illustrative of potential risks rather than realistic clinical predictions. This behavior represents a simplified assumption and does not reflect real-world clinical decision-making processes or triage practices, which are far more complex and guided by medical expertise. Therefore, outcomes observed under healthcare saturation should be interpreted as a modeling limitation rather than a clinically accurate prediction.

Flexibility was also enhanced by introducing parameters to control the number of provinces and the mobility behavior of individuals. A new parameter, called Same Province Percentage (*SPP*), allows control over the proportion of individuals whose destination province

matches their origin. For instance, setting *SPP* to 80% models low inter-province mobility, useful for rural or disconnected regions, while a lower *SPP* simulates high urban mobility, such as between neighborhoods in a city. This parameter, combined with the ability to vary the number of individuals and provinces, results in a highly adaptable simulation environment suitable for diverse scenarios.

Generalization of infections

Another major generalization concerns the type of infection being modeled. While this work focuses on COVID-19, the simulator is designed to be adaptable to other infectious diseases. The two base models used diverged significantly in infection dynamics: LOIMOS employed a viral load model with high granularity, while MVT used a simplified fixed-day cycle (Incubation → Infected → Recovered).

To accommodate various infection types, TEAM includes support for both approaches. This flexibility is crucial when modeling novel diseases where detailed clinical parameters may not yet be available.

Additional modularity is provided by enabling or disabling components such as ICUs. While critical for COVID-19 simulations, ICUs may be irrelevant for diseases with low hospitalization rates. The simulator can also incorporate confinement policies. By setting parameters for start time and duration, scenarios involving time-specific lockdowns can be tested to determine optimal containment strategies.

Another important element is the Prudence Parameter (*PP*), which allows the simulation to reflect varying levels of public awareness and responsiveness. For a well-known disease with visible symptoms and public warnings, a high *PP* simulates a population acting prudently. Conversely, for a new disease with ambiguous or mild symptoms, a low *PP* represents delayed recognition and high unintentional transmission, capturing important epidemiological dynamics. In such scenarios, individuals may become unwitting vectors, mistaking mild symptoms for unrelated or negligible conditions, and continue interacting socially, thereby facilitating the spread of the disease [41]. These features collectively make TEAM highly generalizable and applicable to a wide range of infectious disease models beyond COVID-19.

Database

Model calibration and result validation constitute a key part of this work. While many simulation parameters were derived from existing models, their integration into a unified framework initially produced results with unrealistically high numbers of infections and deaths. This discrepancy became evident when comparing simulation outputs with empirical data from the Lombardy region, which had not been previously used as a validation benchmark.

In particular, LOIMOS produces a combined infection peak of roughly 46% (summing across the four infection types). This high value can be largely attributed to the absence of explicit intervention mechanisms and limited modeling of adaptive behavioral responses, resulting in a scenario where individuals continue their regular activities despite the spread of the disease. Under such assumptions, the model captures a worst-case epidemic trajectory in which the infection spreads largely unchecked across the population.

By contrast, MVT yields prevalence peaks between 8% and 20%, depending on the value of the caution factor. The integration of the two approaches therefore required careful parameter calibration, together with the introduction of behavioral and intervention-related mechanisms, in order to obtain more realistic epidemic trajectories.

Parameter tuning focused on epidemiological factors such as transmission probability, viral progression, and mortality rates conditional on individual health and symptom profiles. These parameters were refined to align model outputs with real-world observations. To ground the validation process, we used the publicly available dataset for the

² F. Reiff and S. Erba, *TEAM: Transmission of Epidemic Among Membranes*, GitHub repository, 2025. Available at: <https://github.com/francireiff/TEAM>.

Lombardy region³, covering the period from February 2020 onward. Lombardy, one of the Italian regions most severely affected during the early phase of the COVID-19 pandemic [42], offers detailed and high-quality data, which have been used extensively in previous studies [43–45]. The model was calibrated primarily against two critical indicators: the number of infected individuals and the number of deaths.

The primary calibration of our model was performed against data from the Lombardy region. However, to ensure the model principles were not narrowly tailored to a single dataset, we conducted a secondary validation using the distinct demographic and epidemiological landscape of Veneto. Using data from Italy’s Civil Protection Department, we re-scaled the simulation for Veneto’s smaller population. This meant modeling a population of 12,000 individuals across the region’s 7 provinces, maintaining the proportional representation used in the Lombardy setup. This test confirmed the robustness of the model. In the 200-day runs, the simulation once again successfully captured the primary infection peak and mirrored the overall trend of cumulative deaths, providing strong evidence that our framework is adaptable and can generalize to different regional contexts.

Pseudocode. Algorithm 1 describes the pseudocode, structured into two main functions:

- **create_scenario()**: Initializes the environment by generating provinces, places, and individuals with the correct demographic distribution. Initial infections are also introduced.
- **run_simulation(days, hours per day)**: Governs the epidemic progression, handling mobility (with probability shown in Table 6), infections, health status updates, hospitalizations, and data recording.

Algorithm 1 Pseudocode of the TEAM simulator

Input: Simulation parameters, days, population
Output: Epidemic evolution data, seconds

```

1: function CREATE_SCENARIO
2:   for all province in provinces do
3:     Create province membrane instance
4:     Calculate the correct number of place membranes
5:     Generate place membranes
6:     Create individuals with the correct age distribution
7:     Assign individuals to houses
8:     Introduce initial infections
9:   end for
10: end function

11: function RUN_SIMULATION(days, hours per day)
12:   Create CSV file
13:   for all day in days do
14:     for all hour in hours per day do
15:       if not a lockdown day and is the correct hour then
16:         Move individuals between provinces through common areas
17:         Move workers to workplaces
18:         Move students to schools
19:         Move elderly to leisure centers
20:         Simulate infections in all places with individuals
21:         Move individuals back home
22:       end if
23:       Trigger infection and vaccination progress
24:       Check for deaths
25:       Discharge recovered individuals from hospitals
26:       Check for hospitalization based on hospital capacity
27:       Track infections and update the scenario
28:     end for
29:     Reduce recovery days in hospitalized individuals
30:   end for
31:   Write data to CSV file and create charts
32: end function

```

³ [giodecris, COVID-19 Regional Data — Italia, 2020](https://github.com/pcm-dpc/COVID-19/tree/master/dati-regioni). Available at: <https://github.com/pcm-dpc/COVID-19/tree/master/dati-regioni>. Accessed 20 Jan 2025.

4. Validation of the model

All graphs in this section report mean values over six simulation runs with $PP = 0.9$ and $SPP = 0.8$, where not specified differently. The plots display the number of susceptible individuals (class S), the disease prevalence (classes E, I, J_1, J_2), the number of recovered individuals (class R), and the number of deaths, according to the information reported in [46].

Here we evaluate the effect of the newly introduced Prudence Parameter (PP), with $0 \leq PP \leq 1$, which controls the probability that symptomatic individuals choose to self-isolate rather than follow their daily routines. The parameter modulates individual behavior in a simple yet effective way: when individuals experience mild symptoms (sym^2), the probability of leaving the house is reduced by a factor of $(1 - PP)^2$. Thus, a higher PP reflects a more cautious population. For instance, if $PP = 0.3$, individuals are about 50% less likely to go out while symptomatic compared to their asymptomatic behavior.

At the extremes, $PP = 0$ corresponds to a population entirely unaware of or indifferent to the disease, resulting in no behavioral change. In contrast, $PP = 1$ models complete prudence, where symptomatic individuals never leave the house, mimicking the original LOIMOS behavior in which infected individuals are fully isolated upon symptom onset.

This parameter can also be interpreted from a sociological perspective. It offers a way to simulate varying levels of civic awareness and compliance with public health guidelines. Even in contexts where information about the disease is widely available, populations may exhibit limited adherence to testing and isolation directives, especially if institutional trust or civic engagement is low [47]. Such behavior has been documented in the Italian situation, as described in [48,49]. As a result, simulations may justifiably adopt medium or low values of PP , even under well-informed conditions.

The impact of PP is illustrated in Fig. 2, which shows the prevalence and deaths under varying values. Simulations with $PP = 0$ were excluded, as they represent implausible scenarios in which no individual, regardless of age or symptom severity, modifies their behavior when symptomatic.

Results demonstrate that PP has a pronounced influence on epidemic dynamics. Lower values lead to unrealistically high peaks in both prevalence and mortality, deviating significantly from real-world data such as that observed in Lombardy and Veneto. In particular, PP values below 0.75 yield outcomes that are inconsistent with known epidemiological patterns, suggesting that models using such parameters may not reflect realistic human behavior during an outbreak.

For this reason, the default value used throughout the rest of the study is $PP = 0.9$, consistent with assumptions made in LOIMOS, which implicitly modeled behavior close to $PP = 1$. It is worth noting that symptom onset does not occur immediately after infection; thus, even high PP values do not eliminate the risk of transmission from individuals unaware of their infectious status.

Note that this current formulation of the parameter PP should be regarded as a high-level simplification, like an umbrella variable that condenses many heterogeneous influences into a single dimension. Nonetheless, the experiments underscore the importance of behavioral response in epidemic containment. They also suggest that promoting voluntary self-isolation in response to symptoms can significantly mitigate disease spread and reduce mortality.

At this point, we present a comparative analysis of three scenarios in which the only varying factor is the lockdown scheduling, while all other parameters remain unchanged. The goal is to evaluate how different confinement measures affect the disease progression.

Lockdowns are among the most effective measures available to contain epidemics. While they do not offer a definitive solution, they can substantially reduce transmission, ease hospital burden, and buy time for medical response. However, prolonged lockdowns are costly from both economic and psychological standpoints. For this reason, it

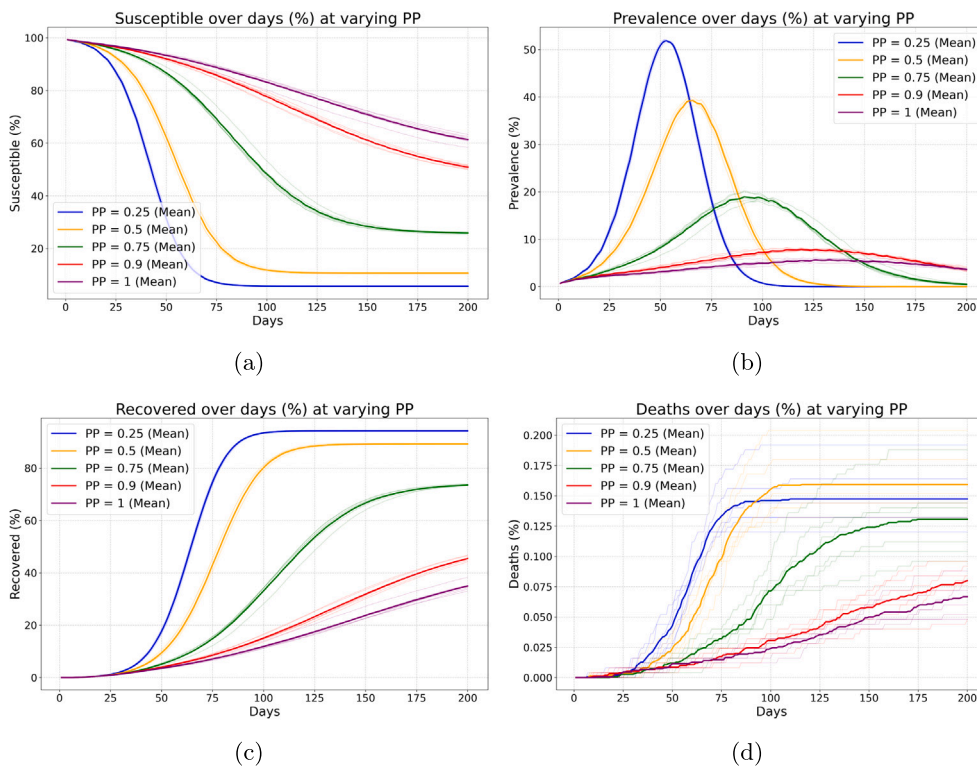


Fig. 2. Validation against PP. Variation in time of susceptible (a), prevalence (b), recovered (c) and deaths (d) according to different values of the parameter PP.

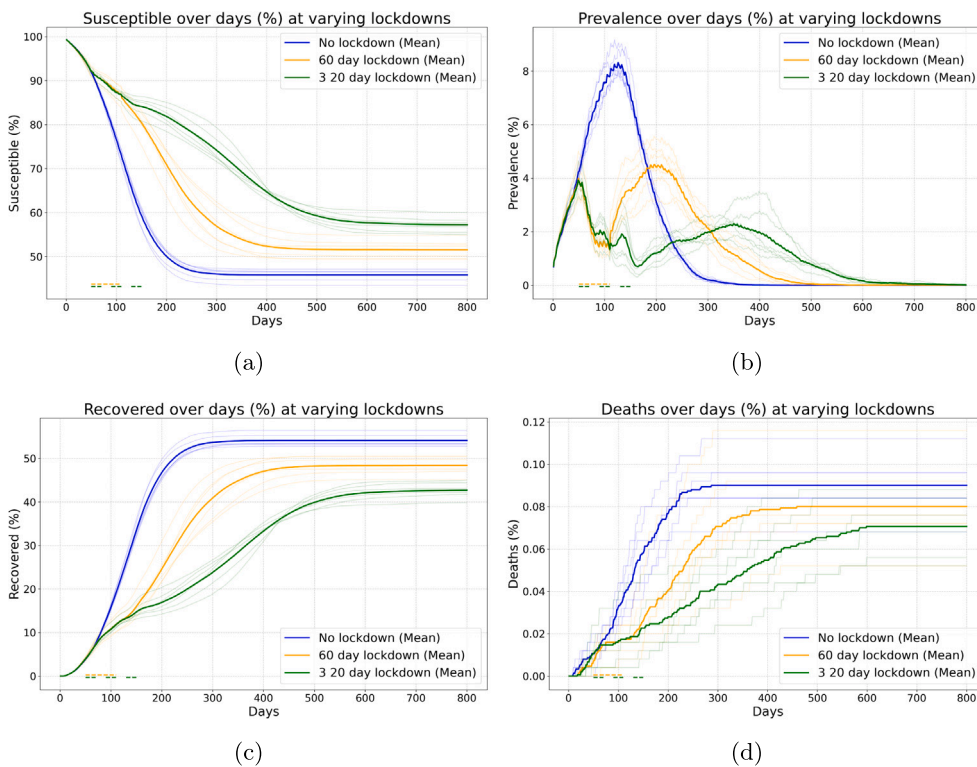


Fig. 3. Validation against targeted lockdowns. Variation in time of susceptible (a), prevalence (b), recovered (c) and deaths (d) according to different lockdown periods.

is crucial to apply them as efficiently as possible, maximizing impact with minimal duration.

Fig. 3 shows three approaches. The first includes no intervention and serves as the baseline. In the second approach, a 60-day lockdown

starts on day 50, aligned with the rising edge of the infection peak. This leads to a significant drop in active cases, which climb again after restrictions are lifted but remain below the values observed without intervention. This confirms that a well-timed lockdown can mitigate

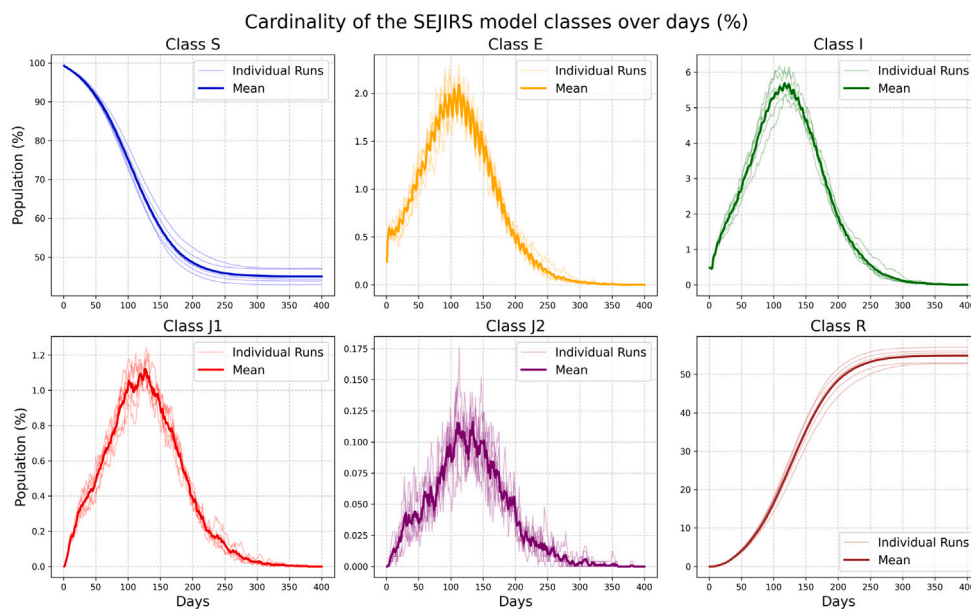


Fig. 4. Cardinality on SEJIRS model. Each subgraph represents the variation in the cardinality of each class in the SEJIRS model, with $PP = 0.9$ and $SPP = 0.8$.

the epidemic's peak and delay its resurgence. The duration of the lockdown is consistent with the first COVID-19 wave in Italy, where strict nationwide restrictions were enforced from March 9, 2020 until early May 2020 [50].

The third approach implements an intermittent confinement strategy, consisting of three 20-day lockdown periods separated by 20-day reopening intervals. Although the total duration of restrictions remains 60 days, the resulting dynamics differ significantly from the single continuous lockdown. The first lockdown rapidly reduces the prevalence to levels comparable to the beginning of the simulation. Interestingly, this downward trend continues even during the subsequent reopening phase, suggesting a delayed effect of the intervention. However, after the second lockdown, the prevalence began to rise again, but was then mitigated by the third lockdown. Following the final reopening, the prevalence increases moderately, and it stabilizes around approximately 2% before gradually declining over time. Overall, each intervention contributes to delaying and lowering the infection peak, effectively flattening the curve in successive stages. However, this strategy also prolongs the duration of the epidemic, extending the period during which the disease remains present in the population.

In the mortality plot, the results exhibit some variability, as the absolute number of deaths remains relatively low and small fluctuations can significantly affect the outcome. This variability is particularly evident in the simulations with a 60-day lockdown, where some runs show higher mortality and others lower mortality compared to the no-lockdown scenario. Therefore, while the differences between strategies are evident, they should be interpreted with caution.

Now, we validate the epidemiological behavior of the model by analyzing the evolution of the SEJIRS compartments over time. Fig. 4 reports the percentage of individuals in each class, averaged over six simulation runs.

The results exhibit the expected dynamics of compartmental epidemic models. The infected population (class I) follows a typical growth-and-decline pattern, reaching a peak before rapidly decreasing, while the susceptible (class S) and recovered (class R) classes show complementary trends. Although short-term fluctuations are present due to the stochastic nature of the model, the overall trends remain stable and clearly identifiable when observed over longer time scales. After the peak, the system gradually approaches a steady state, with most compartments stabilizing and transitions between classes becoming less pronounced.

Finally, the impact of the Same Province Percentage (SPP), with $0 \leq SPP \leq 1$, is evaluated. This parameter represents the fraction of individuals whose daily movements remain within their province of origin. So, $SPP = 0$ corresponds to a population that moves between provinces every day, while $SPP = 1$ models complete isolation between provinces. This parameter provides a flexible way to represent different spatial granularities, from highly interconnected regions to fully separated areas, such as neighborhoods or small communities.

Fig. 5 shows the results obtained for different values of SPP . Compared to other parameters, its effect on the epidemic dynamics is more moderate. In general, higher values of SPP tend to reduce the number of infected individuals, as mobility between provinces decreases and opportunities for cross-area transmission are limited.

Overall, the results suggest that limiting inter-provincial movement can contribute to reducing disease spread, although its impact is less pronounced compared to behavioral or policy-driven interventions.

5. Conclusions

This work investigated the application of P systems to the simulation of infectious disease dynamics. The main objective achieved was the combination of two key aspects, behavioral management and infection diffusion complexity, into a single coherent framework.

A major strength of P systems lies in their natural support for parallel computation, which facilitates efficient large-scale simulations while preserving modularity and adaptability. However, it is important to note that this parallelism is not exploited in the current implementation of TEAM, which relies on a sequential execution of the model. In this work, several features were implemented to generalize the model to various epidemiological scenarios. Among these are the dynamic configuration of provinces and place membranes, the Same Province Percentage (SPP) parameter, controlling mobility patterns, and parameters such as the Prudence Parameter (PP) for behavioral responses, and optional inclusion of ICUs, and viral-load-based infection dynamics.

These features allow TEAM to reproduce complex disease dynamics, including the effects of individual awareness, government interventions, and structural healthcare components. A graphical interface was also developed to ensure usability and support further experimentation.

Simulations were conducted under a range of settings: 25,000 individuals, 12 provinces, and different day durations, where behavioral

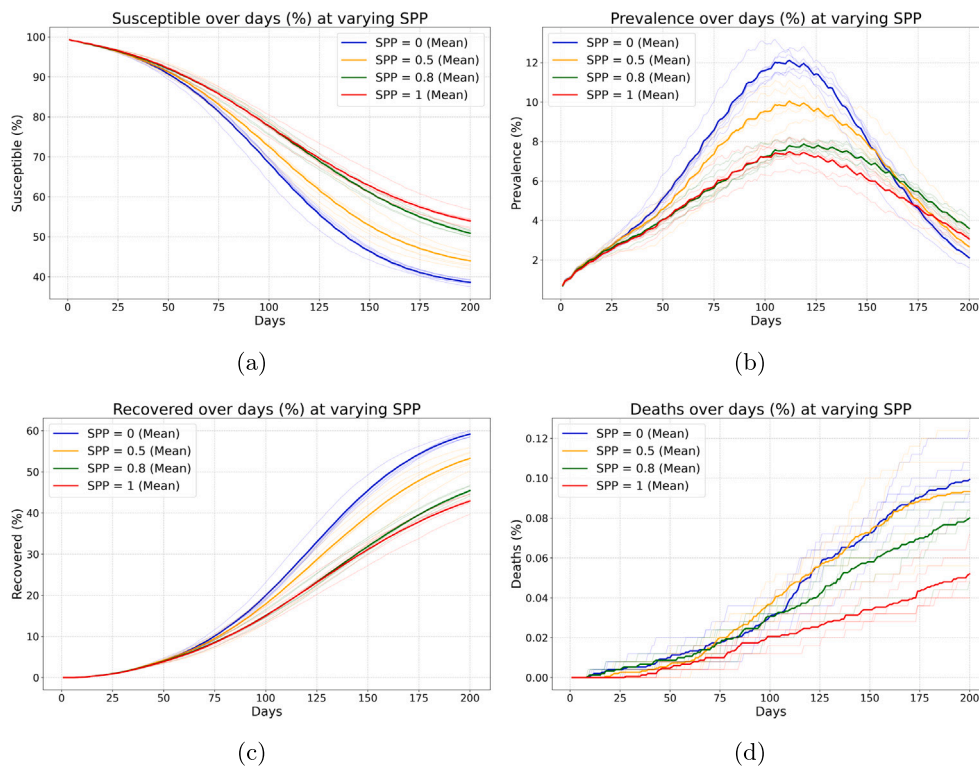


Fig. 5. Validation against SPP. Variation in time of susceptible (a), prevalence (b), recovered (c) and deaths (d) according to different values of the parameter SPP.

elements and lockdowns were tested. The results were confirmed about (i) the relevance of parameters like PP and SPP to shape the observed dynamics, (ii) the evolution of the epidemiological compartments during the simulation runs, and (iii) the cruciality of confinement intervention to significantly impact infection spread. The above validates the model's potential as a decision-support tool. Regional data, particularly from Lombardy and Veneto, were employed in two different tranches of validation,⁴ confirming the system's ability to reflect realistic epidemic curves.

To further enhance the model's realism and adaptability, several research directions are envisaged. Parameters related to prudence, infection dynamics, daily schedules, and mobility across place membranes were calibrated specifically for some regions of the Italian context, as mentioned. It has been our starting point, given the availability of detailed datasets. A natural next step will be to test the simulator on other countries and contexts, to increase its generalization and confirm that the included variables can capture diverse population behaviors.

Another relevant direction concerns the refinement of the infection dynamics. In particular, future work could explore alternative formulations that decouple symptom progression from viral load dynamics, in order to better align the model with current clinical understanding.

Demographic factors such as births and non-disease-related deaths could be integrated, which would allow for more realistic long-term simulations, accounting for population turnover. Improvements of computational performance could also be achieved by parallelizing the

simulation, enabling faster execution, especially in large-scale or long-duration scenarios.

Regarding the Prudence Parameter, while its current formulation as a high-level simplification is effective for modeling purposes, a deeper behavioral and sociological refinement could substantially increase the realism of the simulations without additional computational complexity. A promising direction for future work is the development of a lightweight database that collects country-specific indicators and suggests plausible values – or ranges – for PP and similar behavioral parameters. Such an extension would enhance the model ability to represent diverse populations and improve its applicability across different epidemiological and cultural contexts.

Incorporating seasonal variations, such as changes in behavior during holidays or colder months, would improve the accuracy of infection and mobility patterns. Further differentiation of household structures, for instance by modeling single-person homes or student residences, could refine transmission dynamics within domestic environments.

The expansion of place membranes, including specific environments like universities or transport hubs, would support more granular simulations. Additionally, simulating travel restrictions between provinces may offer insights into the effectiveness of regional containment strategies.

Finally, applying optimization techniques or machine learning could support parameter tuning and predictive accuracy, while testing the model against data from different infectious diseases would assess its generality, flexibility, and robustness.

Although the current model incorporates several real life features and enjoys reliable dynamics and good simulation performance, we are aware that our analysis of the infection diffusion remains primarily qualitative and scenario-based. Future developments in this direction will focus on enhancing analytical rigor through systematic sensitivity analyses, ensuring that conclusions are robust across a broader range of parameter spaces and not overly dependent on specific initial settings.

In conclusion, TEAM combines epidemiological depth and behavioral flexibility, providing a strong foundation for further research in disease modeling and public health management strategy.

⁴ A project carried out across two theses, both available at <https://github.com/francireiff/TEAM>: (i) S. Erba, *Covid-19 infection inspired diffusion dynamics: Generalization of a membrane-based simulator*, MSc Thesis, Department of Computer Systems and Communication, University of Milano-Bicocca, 2025 and (ii) F. Reiff, *A Membrane System Simulator for Covid-19 Infection Diffusion*, Bachelor Thesis in Bioinformatics, Department of Informatics, University of Verona, 2025

CRedit authorship contribution statement

Sandro Erba: Writing – review & editing, Writing – original draft, Software, Project administration, Methodology, Investigation, Data curation, Conceptualization. **Giuditta Franco:** Writing – review & editing, Validation, Methodology, Funding acquisition. **Francesco Reiff:** Writing – original draft, Software, Investigation, Data curation. **José M. Sempere:** Writing – review & editing, Validation, Methodology, Funding acquisition. **Claudio Zandron:** Writing – review & editing, Validation, Methodology, Funding acquisition.

AI-use disclosure

The authors used generative AI tools solely to improve the clarity and readability of the manuscript text. All AI-assisted outputs were carefully reviewed, edited, and validated by the authors. No AI tools were used to generate, modify, or analyze scientific data, results, figures, or any other substantive research content. The authors take full responsibility for the content of this work.

Statements

We hereby confirm that this manuscript is an original unpublished work and the manuscript or any variation of it has not been submitted simultaneously elsewhere, all authors have checked the manuscript and have agreed to the submission, and we have no conflicts of interest to disclose.

Funding

Sandro Erba was funded by the Department of Computer Science, University of Verona, within the project *Application of SN P systems to the federated learning of biomedical data* FUR_FRANCO - UA.VR.050.DPINF.DINF-RATE.

José M. Sempere was funded by the Generalitat Valenciana, Spain within the Prometeo program in the project *A disruptive way to ameliorate the diagnosis and treatment of sensorineural diseases*. CIPROM/2023/026.

Claudio Zandron was partially supported by the MUR (Ministero dell'Università e della Ricerca) under the grant “Dipartimenti di Eccellenza 2023-2027” of the Department of Informatics, Systems and Communication (DISCo) of the University of Milano-Bicocca, Italy.

Declaration of competing interest

The authors declare the following financial interests/personal relationships which may be considered as potential competing interests: Sandro Erba reports financial support was provided by University of Verona Department of Computer Science. Jose M. Sempere reports financial support was provided by Generalitat of Valencia. If there are other authors, they declare that they have no known competing financial interests or personal relationships that could have appeared to influence the work reported in this paper.

Acknowledgments

We all wish to thank Marcelino Campos from Universitat Politècnica de València, who is the developer of LOIMOS, for fruitful discussions with him about the software details implementing modeling approaches of LOIMOS.

Data availability

The source code of the simulator, together with the scripts used to generate the figures presented in this work, is publicly available (F. Reiff and S. Erba, *TEAM: Transmission of Epidemic Among Membranes*, GitHub repository, 2025. Available at: <https://github.com/francireiff/TEAM>). The exact version of the code used for the experiments corresponds to commit d5234e5, dated 23/04/2026. All simulation outputs used to produce the figures (in CSV format), as well as the script `plot_generator.py` used for data visualization, are included in the repository. Simulations are configured through the GUI, which automatically generates a text file containing the full list of parameters and their values for each run. A baseline configuration file, called `baseline_simulator_parameters.txt`, is provided, containing the default set of parameters used across all simulations. For each experiment, only a subset of parameters (e.g., *PP*, *SPP*, and lockdown schedules) is varied, while all other parameters remain unchanged. Input data for regional calibration (e.g., Lombardy and Veneto) were obtained from the [Italian Civil Protection Department repository](#), accessed in 2025. All experiments were performed using Python 3.12.3 within a virtual environment. The required dependencies are listed in the `requirements.txt` file included in the repository. Results are obtained from multiple simulation runs using different random seeds (1, 2, 3, 42, 999, 1234). The provided data and scripts allow full reproduction of the figures presented in this work.

References

- [1] S Verlan. Using the formal framework for P systems. In: International Conference on Membrane Computing. Springer; 2013, p. 56–79. http://dx.doi.org/10.1007/978-3-642-54239-8_6.
- [2] Freund R, Verlan S. A formal framework for static (tissue) p systems. In: International workshop on membrane computing. Springer; 2007, p. 271–84. http://dx.doi.org/10.1007/978-3-540-77312-2_17.
- [3] Freund R, I Pérez-Hurtado, Riscos-Núñez A, et al. A formalization of membrane systems with dynamically evolving structures. *Int J Comput Math* 2013;90(4):801–15. <http://dx.doi.org/10.1080/00207160.2012.748899>.
- [4] Manca V, Castellini A, Franco G, et al. Metabolic p systems: A discrete model for biological dynamics. *Chin J Electron* 2013;22(4):717–23, <https://ieeexplore.ieee.org/abstract/document/10285821>.
- [5] Păun G. Computing with membranes. *J Comput System Sci* 2000;61(1):108–43. <http://dx.doi.org/10.1006/jcss.1999.1693>.
- [6] Păun G. Membrane computing: an introduction. Springer Verlag Berlin; 2002, <http://dx.doi.org/10.1007/978-3-642-56196-2>.
- [7] Franco G, Jonoska N, Osborn B, et al. Knee joint injury and repair modeled by membrane systems. *BioSystems* 2008;91(3):473–88. <http://dx.doi.org/10.1016/j.biosystems.2007.02.010>.
- [8] A Paun. On P systems with active membranes. In: UMC. Springer; 2000, p. 187–201. http://dx.doi.org/10.1007/978-1-4471-0313-4_15.
- [9] C Zandron. Bounding the space in P systems with active membranes. *J Membr Comput* 2020;2(2):137–45. <http://dx.doi.org/10.1007/s41965-020-00039-x>.
- [10] Zandron C, Leporati A, Ferretti C, et al. On the computational efficiency of polarizationless recognizer p systems with strong division and dissolution. *Fund Inform* 2008;87(1):79–91, <https://journals.sagepub.com/doi/abs/10.3233/FUN-2008-87106>.
- [11] Ciobanu G. Scalable distributed implementation of a biologically inspired parallel model. *Complex Intell Syst* 2015;1(1):69–80. <http://dx.doi.org/10.1007/s40747-015-0003-3>.
- [12] Zandron C, Ferretti C, Mauri G. Solving NP-complete problems using p systems with active membranes. In: Unconventional models of computation, uMC'2K: proceedings of the second international conference on unconventional models of computation, (uMC'2K). Springer; 2001, p. 289–301. http://dx.doi.org/10.1007/978-1-4471-0313-4_21.
- [13] Pan L, Alhazov A. Solving HPP and SAT by p systems with active membranes and separation rules. *Acta Inform* 2006;43:131–45. <http://dx.doi.org/10.1007/s00236-006-0018-8>.
- [14] Baquero F, Campos M, Llorens C, et al. P systems in the time of COVID-19. *J Membr Comput* 2021;3:246–57. <http://dx.doi.org/10.1007/s41965-021-00083-1>.
- [15] Valcamonica D, A D'Onofrio, Fareed M, et al. A dynamic behavior epidemiological model by membrane systems. *J Membr Comput* 2025;7:266–80. <http://dx.doi.org/10.1007/s41965-025-00188-x>.
- [16] Campos M, Sempere JM, JC Galán, et al. Simulating the efficacy of vaccines on the epidemiological dynamics of SARS-CoV-2 in a membrane computing model. *3, Microlife*; 2022, <http://dx.doi.org/10.1093/femsm/uaq018>, uaq018.

- [17] Campos M, Llorens C, Sempere JM, et al. A membrane computing simulator of trans-hierarchical antibiotic resistance evolution dynamics in nested ecological compartments (ARES). *Biology Direct* 2015;10(1):41. <http://dx.doi.org/10.1186/s13062-015-0070-9>.
- [18] Colomer MÀ Margalida A, F Alòs, et al. Modeling of vaccination and contact tracing as tools to control the COVID-19 outbreak in Spain. *Vaccines* 2021;9(4):386. <http://dx.doi.org/10.3390/vaccines9040386>.
- [19] Campos M, Sempere JM, JC Galán, et al. Simulating the impact of non-pharmaceutical interventions limiting transmission in COVID-19 epidemics using a membrane computing model. 2, *MicroLife*; 2021, <http://dx.doi.org/10.1093/femsm/luqab011>, uqab011.
- [20] Ryan M, Brindal E, Roberts M, et al. A behaviour and disease transmission model: incorporating the health belief model for human behaviour into a simple transmission model. *J R Soc Interface* 2024;21(215):20240038. <http://dx.doi.org/10.1098/rsif.2024.0038>.
- [21] A D'Onofrio, Fareed MM, Franco G, et al. Integrating human behavior and membrane computing in epidemiological models. 2025, [Submitted].
- [22] Zhang X, Wang J, Yu C, et al. Agent-based modeling of epidemics: approaches, applications, and future directions. *Technologies* 2025;13(7). <http://dx.doi.org/10.3390/technologies13070272>.
- [23] Steinhöfel K, Heslop D, MacIntyre C. Agent-based models of virus infection. *Curr Clin Microbiol Rep* 2025;12(1). <http://dx.doi.org/10.1007/s40588-024-00238-5>.
- [24] Eden M, Castonguay R, Munkhbat B, et al. Agent-based evolving network modeling: a new simulation method for modeling low prevalence infectious diseases. *Health Care Management Sci* 2021;24(3):623–39. <http://dx.doi.org/10.1007/s10729-021-09558-0>.
- [25] Sun Z, Bai R, Bai Z. The application of simulation methods during the COVID-19 pandemic: A scoping review. *J Biomed Inform* 2023;148:104543. <http://dx.doi.org/10.1016/j.jbi.2023.104543>.
- [26] Kabir K, Tanimoto J. Assessing the instantaneous social dilemma on social distancing attitudes and vaccine behavior in disease control. *Sci Rep* 2024;14(1):14244. <http://dx.doi.org/10.1038/s41598-024-64143-z>.
- [27] Tanimoto J. In: *Sociophysics approach to epidemics*, vol. 23, Springer; 2021, <http://dx.doi.org/10.1007/978-981-33-6481-3>.
- [28] Elsayed AA, R Ceprián, Hafez AI, et al. Enhancing p systems for complex biological simulations. *Appl Sci* 2026;16(2). <http://dx.doi.org/10.3390/app16020705>.
- [29] JN Davidson. William Ogilvy Kermack 1898–1970. *Biograph Memoirs Fellows Royal Soc* 1971;17:399–429. <http://dx.doi.org/10.1098/rsbm.1971.0015>.
- [30] F Brauer. Compartmental models in epidemiology. In: *Mathematical epidemiology*. Springer; 2008, p. 19–79. http://dx.doi.org/10.1007/978-3-540-78911-6_2.
- [31] C Vargas-De-León. On the global stability of SIS, SIR and SIRS epidemic models with standard incidence. *Chaos Solitons Fractals* 2011;44(12):1106–10. <http://dx.doi.org/10.1016/j.chaos.2011.09.002>.
- [32] Bame N, Bowong S, Mbang J, et al. Global stability analysis for SEIS models with n latent classes. *Math Biosci Eng* 2008;5(1):20–33. <http://dx.doi.org/10.3934/mbe.2008.5.20>.
- [33] Wan H, et al. An SEIS epidemic model with transport-related infection. *J Theoret Biol* 2007;247(3):507–24. <http://dx.doi.org/10.1016/j.jtbi.2007.03.032>.
- [34] ON Bjørnstad, Shea K, Krzywinski M, et al. The SEIRS model for infectious disease dynamics. *Nature Methods* 2020;17(6):557–9. <http://dx.doi.org/10.1038/s41592-020-0856-2>.
- [35] Gumel AB, Ruan S, Day T, et al. Modelling strategies for controlling SARS outbreaks. *Proc R Soc Lond [Biol]* 2004;271(1554):2223–32. <http://dx.doi.org/10.1098/rspb.2004.2800>.
- [36] Giordano G, Blanchini F, Bruno R, et al. A SIDARTHE model of COVID-19 epidemic in Italy. 2020, <http://dx.doi.org/10.48550/arXiv.2003.09861>, arXiv preprint. [arXiv:200309861](https://arxiv.org/abs/200309861).
- [37] Giordano G, Blanchini F, Bruno R, et al. Modelling the COVID-19 epidemic and implementation of population-wide interventions in Italy. *Nature Med* 2020;26(6):855–60. <http://dx.doi.org/10.1038/s41591-020-0883-7>.
- [38] Higazy M. Novel fractional order SIDARTHE mathematical model of COVID-19 pandemic. *Chaos Solitons Fractals* 2020;138:110007. <http://dx.doi.org/10.1016/j.chaos.2020.110007>.
- [39] Akkilic AN, Sabir Z, Raja MAZ, et al. Numerical treatment on the new fractional-order SIDARTHE COVID-19 pandemic differential model via neural networks. *Eur Phys J Plus* 2022;137(3):334. <http://dx.doi.org/10.1140/epjp/s13360-022-02525-w>.
- [40] Pérez-Hurtado I, Orellana-Martín D, Zhang G, et al. P-lingua in two steps: flexibility and efficiency. *J Membr Comput* 2019;1:93–102. <http://dx.doi.org/10.1007/s41965-019-00014-1>.
- [41] Mowbray F, Woodland L, Smith LE, et al. Is my cough a cold or covid? a qualitative study of COVID-19 symptom recognition and attitudes toward testing in the UK. *Front Public Health* 2021;9:716421. <http://dx.doi.org/10.3389/fpubh.2021.716421>.
- [42] Remuzzi A, Remuzzi G. COVID-19 and Italy: what next?. *Lancet* 2020. [http://dx.doi.org/10.1016/S0140-6736\(20\)30627-9](http://dx.doi.org/10.1016/S0140-6736(20)30627-9).
- [43] Cereda D, Tirani M, Rovida F, et al. The early phase of the COVID-19 outbreak in Lombardy Italy. 2020, <https://arxiv.org/abs/2003.09320>. [arXiv:2003.09320](https://arxiv.org/abs/2003.09320).
- [44] Rovetta A, Bhagavathula A, Castaldo L. Modeling the epidemiological trend and behavior of COVID-19 in Italy. *Cureus* 2020. <http://dx.doi.org/10.7759/cureus.9884>.
- [45] Lombardi A, Amoroso N, Monaco A, et al. Complex network modelling of origin–destination commuting flows for the COVID-19 epidemic spread analysis in Italian Lombardy region. *Appl Sci* 2021;11(10). <http://dx.doi.org/10.3390/app11104381>.
- [46] U Giménez-Mujica, A Anzo-Hernández, J Velázquez-Castro. Epidemic local final size in a metapopulation network as indicator of geographical priority for control strategies in SIR type diseases. *Math Biosci* 2022;343:108730. <http://dx.doi.org/10.1016/j.mbs.2021.108730>.
- [47] Hills S, Eraso Y. Factors associated with non-adherence to social distancing rules during the COVID-19 pandemic: a logistic regression analysis. *BMC Public Health* 2021. <http://dx.doi.org/10.1186/s12889-021-10379-7>.
- [48] Carlucci L, I D'Ambrosio, Balsamo M. Demographic and attitudinal factors of adherence to quarantine guidelines during COVID-19, the Italian model. *Front Psychol* 2020;11. <http://dx.doi.org/10.3389/fpsyg.2020.559288>.
- [49] Webster R, Brooks S, Smith L, et al. How to improve adherence with quarantine: rapid review of the evidence. *Public Health* 2020;182:163–9. <http://dx.doi.org/10.1016/j.puhe.2020.03.007>.
- [50] Silverio A, M Di Maio, Ciccarelli M, et al. Timing of national lockdown and mortality in COVID-19: the Italian experience. *Int J Infect Dis* 2020;100:193–5. <http://dx.doi.org/10.1016/j.ijid.2020.09.006>.

Sandro Erba is a Ph.D. student in computer science at the University of Milano-Bicocca, Italy. He received his master's degree in computer science with a thesis focused on membrane computing applied to epidemiological modeling. His current research interests include P systems, spiking neural networks, natural computing and complex systems simulation.